3D spheroid cultures for evaluation of nanophotosensitizers accumulation

Aleksey Skobeltsin[1], Dina Farrakhova[1], Yulia Maklygina[1], Igor Romanishkin[1], Anastasia Ryabova[1], Ilya Yakovets[3], Marie Millard[3], Lina Bolotine[3], Anna Plyutinskaya[4], Tatyana Karmakova[4], Andrey Pankratov[4], Victor Loschenov[1,2]

[1]Prokhorov General Physics Institute of the Russian Academy of Sciences, Vavilova str.38, Moscow, Russia
[2]National Research Nuclear University «MEPhI», Kashirskoe shosse 31, Moscow, Russia
[3]Centre de Recherche en Automatique de Nancy (CRAN), Université de Lorraine, Institut de Cancérologie de Lorraine, 6 avenue de bourgogne - CS 30519, 54519 Vandoeuvre-les-Nancy Cedex, France
[4]National Medical Research Radiological Centre of the Ministry of Health of the Russian Federation; 3, 2nd Botkinskiy pr., Moscow, 125284, Russia

Abstract. Current paper presents the results of the usage of indocyanine green and pheophorbide nanoform on 2D and 3D models of FaDu cells culture. The 2D model or monolayer was used for investigation of nanoparticles distribution within individual cells and their organelles. The 3D model or multicellular tumor spheroids were used for estimation of cells' metabolic processes by the investigation of the nanophotosensitizers fluorescence distribution within spheroid's layers. It was shown that pheophorbide nanoparticles are accumulated in the external cell layers of spheroids, indocyanine green nanoparticles distribution demonstrates completely opposite status – in the central part of the spheroid.

1. Introduction

The accumulation and distribution of photosensitizers (PS) in the tumor cells is a pivotal value of photodynamic therapy (PDT) efficient. PDT has a number of advantages over conventional methods of cancer treatment: (a) local impact, (b) non-invasiveness and efficacy, especially in surgically untreatable cases, (c) no long-term adverse events compared with chemotherapy, and (d) absence of systemic immunosuppression, as opposed to chemotherapy and ionizing radiation. However, adverse events and significant phototoxicity because of non-specific distribution in the body have encouraged researchers to develop new PSs. Nanoform of PS enhances the selectivity of PS accumulation in tumor cells. The PSs which are often used in clinical practice have an aromatic and hydrophobic structure with poor or limited solubility in water. This fact indicates a tendency to aggregation which can lead to incomplete destruction of tumor cells.

Considering PS efficacy, safety, and high potential in the area of theranostics (therapy and diagnostics), many researchers are seeking approaches to improve its characteristics, such as its solubility, phototoxicity, and accumulation in tumors. One of these approaches, which have proved successful in recent years, is supplying the drug with a delivery system. Development of nanotechnologies in the past years has initiated the extension of studies focused on the creation of effective drug delivery systems. The introduction of new materials and technologies enables the design of transport systems using various nanoparticles. For example, several PS delivery systems based on

polymers, gold nanoparticles, carbon nanotubes, silicon nanoparticles, liposomes, etc [1-8]. Unfortunately, these delivery systems have some drawbacks such as low drug loading content and complex preparation method, which significantly decrease the destruction of cancer cells. Nanoparticles reduce the density of hydrophobic PS for aggregation in aqueous media, increase circulation time, and allow passive and active intra-tumor and intracellular delivery of PS. In comparison with typical drug delivery systems, PS nanoform capable produces oxygen molecules without allocation of PS molecules [9]. As opposed to the other delivery systems, they feature properties such as biocompatibility, low toxicity, and variability of structure and physic-chemical properties.

Nanoparticles characterized by the accumulation in the tumor tissue due to the effect of "enhanced penetration and retention", which is characterized by the presence of large pores in the walls of blood vessels due to the presence of incomplete endothelial barrier, defective vascular architecture and impaired lymphatic drainage system of the tumor [10, 11]. For instance, the pores of the vessels of normal tissue are 2-3 nm, and in tumor tissues the pore diameter can reach 500 nm.

Investigated PSs were chosen based on their spectroscopic properties. Pheophorbide in nanoform was chosen as a PS of the red spectral range. Indocyanine green (ICG) in nanoform was chosen as a PS of the infrared spectral range. ICG nanoparticles have the specific properties because of its reconstruction by J-type aggregates with changing optical properties featured by a red-shifted, intense and narrow absorption peak, known as a J-band [12, 13]. ICG nanoparticles (ICG NPs) formed J-aggregates enable to change optical properties by interaction with complex mixtures of proteins, lipids which provide an alteration of the J-aggregate packing arrangement [13]. In biological media, ICG NPs changes its state from an aggregated to a monomeric and it leads to changes in absorption and fluorescence due to binding to serum albumin protein [14]. J-aggregates are the preferable form of PS for head and neck cancer treatment [13].

The estimation of PS distribution allows understanding the behavior of nanoparticles in 2D and 3D tissue models, which help predict *in vivo* PS properties. The cell monolayer is used for evaluation of anticancer drugs and treatments. In this type of model, cells grow on the surface next to one another, which does not reproduce *in vivo* cells environment. 3D tissue models (spheroids) mimic cell-cell interactions in tissues better than cells monolayer. Multicellular spheroids are the most popular 3D model used in cancer research because they display different environmental micro-regions of tumors: a necrotic core (the center), cells at rest, and a proliferating pool (the outer part). This cells arrangement exhibits the morphology reflecting the features of certain types of the early stage solid tumors. In this report, we present the results of nano PSs accumulation and distribution on FaDu spheroids from human squamous cell carcinoma of the hypopharynx. 3D FaDu spheroids are considered as a good model of oral cancer in order to study heterogeneity of this type of tumor by the analysis of the PS accumulation and distribution.

2. Materials and Methods

In the study pheophorbide-a nanoparticles (Pheo NPs) were used such as a PS of red visible spectral range. Pheo NPs were obtained from polycrystalline methyl pheophorbide-a powder. Pheo NPs are colloidal solution of molecular pheophorbide nanocrystals. Polycrystalline powder was added to distilled water with 1 mg/ml concentration. The resulting suspension was dispersed in the ultrasonic homogenizer Bandelin SONOPLUS HD2070. 120÷140 nm average diameter of particles in an aqueous colloid was obtained by multi-angle dynamic light scattering (Photocor Complex). Dimethylsulfoxide (DMSO) was a solvent for the substance. An equal volume of DMSO was added to a pheophorbide-a colloidal solution and absorption spectra were obtained for quantitative determination of concentration. The absorption spectra of samples were obtained via computerized Hitachi U-3400 spectrophotometer (190 – 2500 nm). It was found that both the molecular and colloidal form of the solution have an absorption peak in the far-red region of 650-700 nm. In particular, the investigated nano-form has a pronounced absorption peak at a wavelength of 675 nm, which confirms its prospects for use as a far-red spectral range.

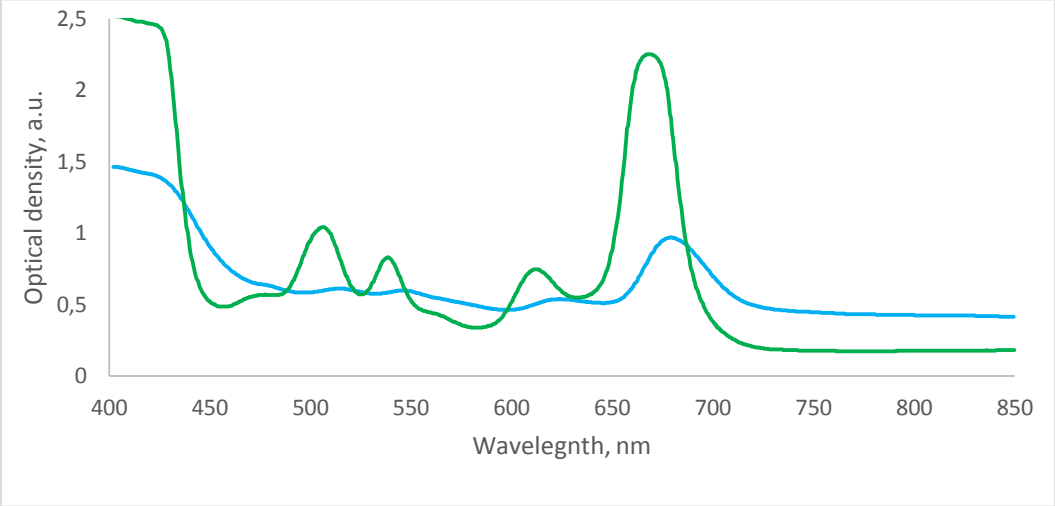

Figure 1. The absorption spectra of Pheo soluble solution and Pheo nanoform.

The colloidal solution of ICG nanoparticles (J-aggregates) based on the polycrystalline powder of the preparation "Cardio-green". This PS appropriate for near IR-range. 1.5 mM ICG aqueous solution was heated in a water bath at 65 °C for 20 hours. After the formation of J-aggregates, the solution was filtered to remove large aggregates. This process was controlled by the Hitachi U-3400 spectrophotometer and the small-angle dynamic light scattering spectrometer Photocor Complex. Finally, the resulting colloidal solution was resuspended in water. Thus, J-aggregates with a 120-140 nm size distribution were obtained. The colloidal solution of J-aggregates was mixed with an equal volume of ethanol changes and absorption spectra were measured to quantify the concentration. The prepared aqueous colloidal solution of ICG J-aggregates has a pronounced absorption peak in the far-red region with a maximum wavelength of 897 nm. Consequently, these properties of ICG NPs makes it is the most promising PS for fluorescent diagnosis of deep-seated tumors.

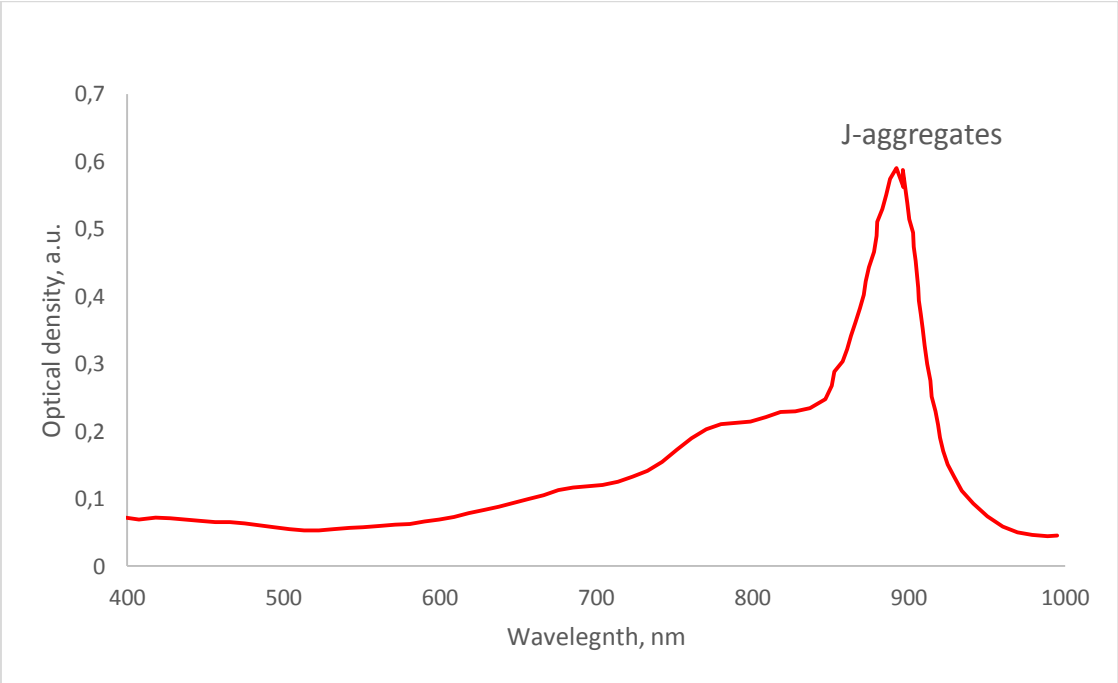

Figure 2. The absorption spectrum of ICG J-aggregates.

The 2D and 3D models of cells were prepared as a SPIE proceeding [15]. The PSs at 5 µg/ml concentration were added to a Petri dish with cell models. The 2D FaDu cell model was incubated with PSs for 120 minutes. The 3D FaDu spheroids were incubated with PSs for 3 hours. The PS distribution study was carried out by confocal microscopy (LSM-710-NLO Carl Zeiss, Germany). Prior to the microscopy study, the spheroids were washed with pre-warmed PBS.

3. Results and Discussion

The microscope images of Pheo NPs fluorescence in FaDu cells at the maximum of accumulation were obtained (fig.3). The maximum of PS fluorescence intensity was observed in 120 minutes after Pheo NPs addition to the Petri dish with FaDu cells. The fluorescence signal was excited by 488 nm for visualization of endogenous fluorophores and 633 nm for exogenous fluorophores. The autofluorescence of FaDu cells was observed in 490-630 nm spectral range [5] while the Pheo NPs fluorescence was observed in 645-800 nm. Pheo NPs accumulated primarily in organelles of cancer cells.

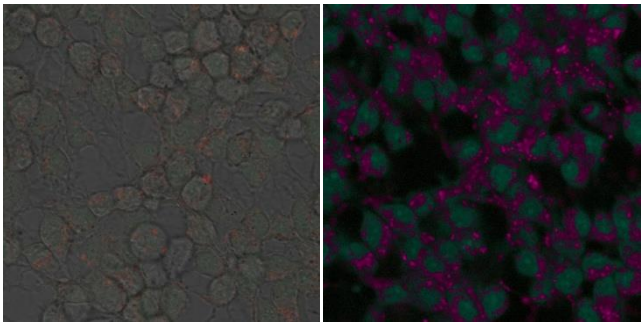

Figure 3. The fluorescence images of FaDu cell monolayer with Pheo NPs.

The microscope images of ICG NPs fluorescence in FaDu cells at the maximum of accumulation were obtained (fig.4a). The fluorescence of ICG NPs in FaDu cells was excited by 488 nm. ICG NPs accumulated primarily in organelles of cancer cells. The fluorescence spectra were obtained from different organelles (the parts pointed by color circles) of FaDu cells (fig.4b).

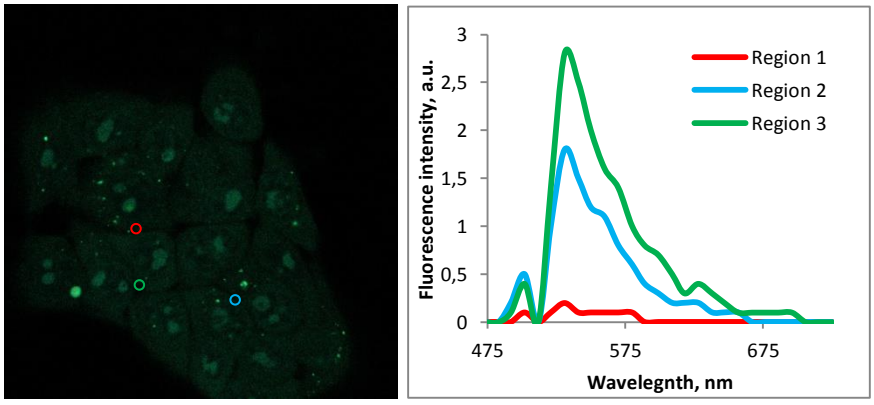

a) b)

Figure 4. a) The fluorescence image of FaDu monolayer with ICG NPs (ex 488 nm), b) The fluorescence spectra of FaDu cell organelles with ICG NPs.

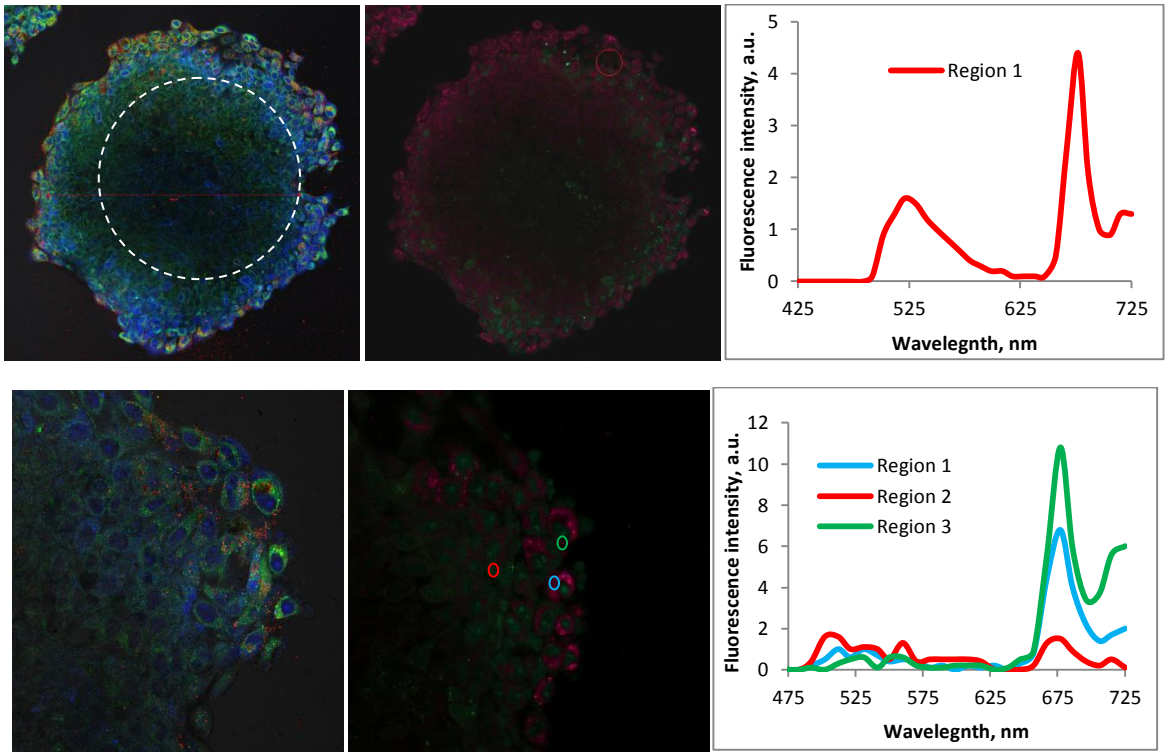

a) b)

Figure 5. The fluorescence images of FaDu spheroid cross section after 3-hour incubation with Pheo NPs, b) The fluorescence spectra of Pheo NPs in FaDu spheroids.

The fluorescence microscopy images of FaDu multicellular tumor spheroid at the maximum of PS incubation (fig.5, 6). The maximum of Pheo NPs fluorescence signal was observed in 3 hours after PS addition. Basically, the Pheo NPs is accumulated in the external cell layers of spheroids. The accumulation of PS was confirmed by fluorescence spectra (fig.5c, 6c). The fluorescence spectrum was obtained from different parts of the external layer of FaDu spheroid. The fluorescence peak at 667 nm corresponds to Pheo NPs fluorescence. The accumulation of Pheo NPs in the proliferating zone of spheroid depends on different rates of cell metabolic processes.

The fluorescence images of tumor spheroids with ICG NPs were obtained. The excitation wavelength was at 514 nm. The fluorescence of ICG NPs is observed in the center part of tumor spheroid which consists of necrotic tissue (fig.6a). The fluorescence spectra were obtained from the internal and external parts of 3D FaDu model. The fluorescence peak at 710 nm in the internal layer confirmed the accumulation of PS in the center of the spheroid (fig.6b).

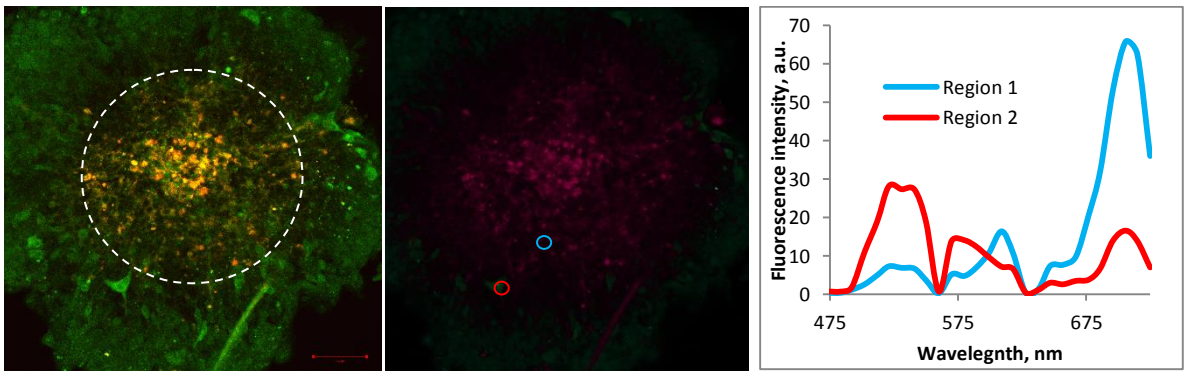

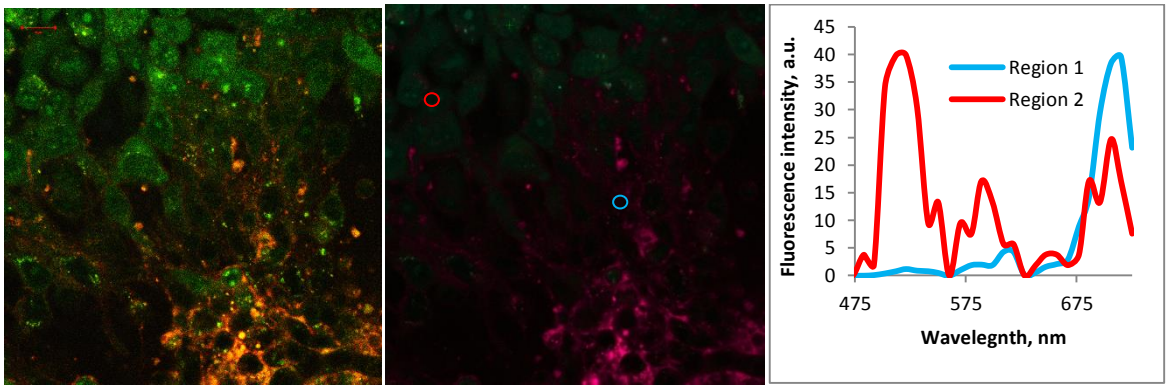

a) b)

Figure 6. The fluorescence images of FaDu spheroid cross section after 3-hour incubation with ICG NPs, b) The fluorescence spectra of ICG NPs in FaDu spheroids.

Thus, the analysis of Pheo NPs accumulation in 2D and 3D tumor cell models allowed demonstrating the accumulation localization of Pheo NPs. Pheo NPs sufficiently homogeneous distributed over the cytoplasm of cells in a two-dimensional cancer model. However, in the case of a three-dimensional model, much more extensive areas of PS accumulation were found at the periphery of the spheroid in comparison to its center. Probably, the presence of this kind of zones is due to different parts of the spheroid are characterized by different metabolism rates. The center of the spheroid is characterized by the presence of a necrotic zone and a non-proliferating cluster of cells. This phenomenon proves the cell localization with fast proliferation in the peripheral base these cells and allows quickly capturing the PS and are accumulated it. Also, these cells capable to prevent PS from deep penetrating into the spheroid. However, for another type of PS such as ICG NPs the completely different picture was observed. Although the uniform intracellular distribution in the monolayer was characterized for this PS type, ICG NPs show an irregular distribution in the three-dimensional cell culture. Although characteristic homogeneous intracellular distribution in the monolayer cell culture was observed, for the three-dimensional cell model, ICG NPs demonstrates an irregular distribution. Basically, the PS accumulation concentrates in the central part of the spheroid, despite significant cell proliferation in the periphery; it does not contribute a significant accumulation of the PS. This fact can be explained by the transition of ICG NPs to the molecular form by dissolving in the biological microenvironment. As a result, the PS in molecular form penetrates significantly into the central part of the spheroid due to the small size of its constituent molecules, and the slow cellular metabolism of the spheroid central part and accumulates in this area, while in the periphery due to fast cellular metabolism is quickly processed and excreted. Noticeably, the advantages of this PS type because it works in the near infrared region of the spectrum, it has a high selectivity characteristic of the nanoform, and at the same time has a rapid elimination, which is uncharacteristic for the nanoform.

4. Conclusion

High accumulation and penetration of PS enhance an amount of dead tumor cells after PDT. This study has shown the penetration ability of nano PSs in *in vitro* avascular models of solid tumors. The nanoform of PSs demonstrated the good properties of accumulation and penetration on the 2D and 3D cells models. The microscopy investigation has shown the different distribution of PSs in the tumor spheroids. Pheo NPs accumulate in the peripheral part of the spheroid, while ICG NPs accumulate in the central area of the spheroid. Consequently, the research pointed to cell metabolism in different parts of spheroids. Consequently, the applying of various PSs can be useful for cancer diagnosis, especially for evaluating the stage of pathogenic tissue and increase the number of dead cells.

Acknowledgments
This work was supported by a Ministry of Science and Higher Education of the Russian Federation - RFMEFI61618X0096.

References
[1.] Chen B, Pogue BW, Hasan T 2005 *Expert Opin Drug Deliv*. **2** 477-87
[2.] Cheng L, Kamkaew A, Sun H, Jiang D, Valdovinos HF, Gong H, et al. 2016 *ACS Nano*. **10** 7721-30
[3.] Hong EJ, Choi DG, Shim MS 2016 *Acta Pharm Sin B*. **6** 297-307
[4.] Lee DJ, Park GY, Oh KT, Oh NM, Kwag DS, Youn YS, et al. 2012 *International Journal of Pharmaceutics*. **434** 257-63
[5.] Medvedeva NV, Prosorovskiy VN, Ignatov DV, Druzilovskaya OS, Kudinov VA, Kasatkina EO, et al. 2015 *Biomed Khim*. **61** 219-30
[6.] Viera L, Castilho M, Ferreira I, Ferreira-Strixino J, Hewitt K, Raniero L 2017 *Photodiagnosis Photodyn Ther*. **18** 6-11
[7.] Wong BS, Yoong SL, Jagusiak A, Panczyk T, Ho HK, Ang WH, et al. 2013 *Advanced Drug Delivery Reviews*. **65** 1964-2015
[8.] Yang H, Chen Y, Chen Z, Geng Y, Xie X, Shen X, et al. 207 *Biomaterials Science*. **5** 1001-13
[9.] Lim C-K, Heo J, Shin S, Jeong K, Seo YH, Jang W-D, et al. 2013 *Cancer Letters*. **334** 176-87
[10.] Maeda H, Nakamura H, Fang J 2013 *Adv Drug Deliv Rev*. **65** 71-9
[11.] Mehraban N, Freeman HS 2015 *Materials*. **8** 4421-56
[12.] Liu R, Tang J, Xu Y, Zhou Y, Dai Z 2017 *Nanotheranostics*. **1** 430-9
[13.] Shakiba M, Ng KK, Huyrih E, Chan H 2017 *Nanoscale*. **8** 12618-25
[14.] Jung B, Vullev VI, Anvari B 2014 *IEEE J Sel Top Quantum Electron*. **20** 149-57
[15.] Farrakhova D, Maklygina Y, Romanishkin I, Ryabova A, Yakavets I, Millard M, et al. 2019 *Saratov Fall Meeting 2018: Optical and Nano-Technologies for Biology and Medicine*. **11065** 1-6